"Gheorghe Asachi" TechnicalUniversity of Iasi, Romania

EFFICIENT REMOVAL OF HEAVY METALS BY KOH ACTIVATED _Diplotaxis harra_ BIOMASS: EXPERIMENTAL DESIGN OPTIMIZATION

Hanane Tounsadi[1,2], Abderrahim Khalidi[2], Meryem Farnane[1], Aicha Machrouhi[1], Alaâeddine Elhalil[1], Noureddine Barka[1*]

[1] _University Sultan Moulay Slimane, Research Group in Environmental Sciences and Applied Materials (SEMA), FP Khouribga, B.P. 145, 25000 Khouribga, Morocco_
[2] _Hassan II University of Casablanca, Faculty of Science and Technology, Laboratory of Physical Chemistry and Bioorganic Chemistry, BP 146, Mohammedia, Morocco_

Abstract

The aim of this study was to produce high quality activated carbons from _Diplotaxis harra_ biomass by potassium hydroxide activation and their application in heavy metals removal. To reduce the number of experiments, full factorial experimental design at two levels (2^4) was carried out to occur optimal preparation conditions for efficient removal of cadmium and cobalt ions from aqueous solutions. Different variables influencing activation process, such as carbonization temperature (500–600°C), activation temperature (400–500°C), activation time (1–2h) and impregnation ratio (g KOH/g carbon) (1–2) have been investigated and the best production conditions were determined. The experimental results showed that the carbonization temperature was the most significant factor that influences the iodine number of the activated carbons. The methylene blue index was more influenced by the activation temperature. The removal of cadmium and cobalt ions by activated carbons was more sensitive to methylene blue index instead of iodine number. Although, the removal of the both heavy metals is more influenced by activation temperature with a negative effect followed by the impregnation ratio with a positive impact. Based to the statistical data, the best conditions for the removal of cadmium and cobalt by the prepared activated carbons have been established. The maximum iodine number and methylene blue index obtained under these conditions were 696.84 mg/g and 235.64 mg/g respectively. The sorption capacities of optimized activated carbons were determined by isotherm study. The maximum capacities obtained with the application of the Langmuir model were 118.09 mg/g for cadmium sorption onto AC carbonized at 600°C, activated at 400°C during 1h with an impregnation ratio of 2 g/g, and 48.89 mg/g for cobalt sorption onto and AC carbonized at 600°C, activated at 500°C during 1h with an impregnation ratio of 2g/g respectively. These sorption capacities were greater than those of a commercial activated carbon used in water treatment.

1. Introduction

Toxic heavy metals represent a major worldwide environmental problem. They are ones of the most serious contaminants in water resulting from manufacturing and mining processes (Zhang et al., 2016a). The metal species can cause various damages to the central nervous system, skin, teeth, liver or lung of human health and serious environmental issues (Ab

Razak et al., 2015; Wu et al., 2014). The rapid development of modern industrial activities suggests the increase of global needs for heavy metals, whereas, environmental regulations on heavy metals are increasingly stringent (Carrillo-Chavez et al., 2014). In order to meet the water and food quality standards, the monitoring of heavy metals in wastewater is necessary. Common techniques are used for the removal of heavy metals from aqueous

---

[*]Author to whom all correspondence should be addressed: e-mail: barkanoureddine@yahoo.fr; Phone: +212661666622; Fax: +21252340354.

solutions like, ion exchange (Ali Fil et al., 2018), membrane filtration (Zhu et al., 2015), coagulation/flocculation (Shak and Wu, 2014), chemical precipitation (Kima et al., 2014), Electrodialytic treatment (Ebbers et al., 2015), electrochemical treatment (Valero et al., 2014) and sorption (Sbaffoni et al., 2018; Teklu et al. 2018). While, sorption process has been widely used due to its high efficiencyand cost-effectiveness. Numerous sorbents have been used to remove heavy metals from wastewater such as clays (Vhahangwele and Mugera, 2015), zeolite (Visa, 2016), nanocomposites (Lofrano et al., 2015), chitosan (Zhang et al, 2016b), polypyrrole (Seid et al., 2014), hydroxyapatite (Barka et al., 2012) and activated carbon (Soylak et al., 1997). Among them, activated carbons are considered to be particularly competitive and effective for the removal of heavy metals because they have outstanding adsorption characteristics due to their improved pore structures, the functional groups present on their surface and their high surface areas. Various lignocellulosic materials like phragmitesaustralis (Guoa et al., 2015), rice husk (Liu et al., 2016), peanut shell (Georgina et al., 2016), tomato waste (Saygili and Güzel, 2016), bamboo (Wang et al., 2015), sargassum (Li et al., 2015), Arundodonax Linn (Chayid and Ahmed, 2015), oak (Jung and Kim, 2014), pineapple waste (Mahamad et al., 2015), tea industry waste (Gundogdu et al., 2012; Gundogdu et al., 2013) and cocoa shell (Saucier et al., 2015) have been used as low-cost precursors for the preparation of this material.

The ability of activated carbons to adsorb pollutants from aqueous solutions depends on two major factors: experimental conditions of the activation processes (Tounsadi et al., 2015) and the nature of starting material utilized for the preparation (Gao et al., 2015). Furthermore, activated carbons can be prepared by physical or chemical activations (Nowicki et al., 2015). In chemical activation, chemical agents are used such as H_3PO_4, $ZnCl_2$, KOH, $NaOH$, H_2SO_4, and K_2CO_3. In physical process, the char produced from carbonization step is activated using a gas as activating agent. Then, oxidation reaction takes place between the carbon atom and the gas, which increases the number of pores in the carbonaceous structure. The production of activated carbon by physical activation requires high temperatures (800–1000°C), which involves high power consumption and a low yield of carbon (Kilpima et al., 2014).

In the chemical activation, the carbonization temperature is varied between 400 and 600°C which significantly reduce the power consumption (Njokua et al., 2014). In addition, the properties of the resulting activated carbon will also be influenced by types of activating reagents, activation time, impregnation conditions, carbonization temperature, and others (Yahya et al., 2015). For that, experimental designs have been used to control the different factors which influence and interfere in the preparation in order to optimize experimental conditions.

This study has focused on the production of activated carbons (ACs) from *Diplotaxis harra* by potassium hydroxide activation. The plant was collected from the region of Khouribga, Morocco. It is a plentiful, easily available, nontoxic and a local known plant. Every year, large amounts of this plant are produced. To investigate the optimal production conditions and to evaluate the ability of these activated carbons to remove heavy metals, a 2^4 full factorial experimental design was used. The factors included in the experimental design were carbonization temperature, activation temperature, activation time and impregnation ratio. Four responses are analyzed, which are; iodine number (IN), methylene blue index (MB index), cadmium and cobalt ions removal efficiency (Cd(II), Co(II)). The ACs produced at the optimal conditions was observed by scanning electron microscopy (SEM).

2. Methodology

2.1. Materials

All the chemicals used in this study were of analytical grade. $Cd(NO_3)_2.4H_2O$ (98%), $Co(NO_3)_2.6H_2O$ (98%), KOH (98%), iodine (I_2), $Na_2S_2O_3.5H_2O$, HCl (37%) and commercial activated charcoal (powder form) were purchased from Sigma-Aldrich (St. Loius, MO, USA). HNO_3 (65%) was provided from Sharlau (Barcelona, Spain). $NaOH$ (99%) from Merck (Darmstadt, Germany), KI was obtained from Pharmac (Casablanca, Morocco) and methylene blue ($C_{16}H_{18}ClN_3S$) (85%) was purchased from Panreac (Barcelona, Spain).

2.2. Preparation of activated carbons

2.2.1. Raw material

The steams of Diplotaxis harra (DH) biomass were selected as a precursor in the preparation of activated carbon because of its availability and desirable physic-chemical characteristics. An elemental or ultimate analysis was performed using a CHNS/O analyzer type Flash 2000 EA 1112 (Thermo Fisher Scientific). Before to the analysis, the samples were dried overnight at 105ºC and cooled in a desiccator. The proximate analysis was applied to define the quantitative measurement of moisture and ash amount. In fact, approximately 2 g (w_1) of powdered Diplotaxis harra was placed into weighed ceramic crucibles. The material was dried at 102°C for 24h and reweighed to obtain the dry powder weight (w_2) and the moisture was calculated by (Eq. 1):

$$Moisture(\%) = \left(\frac{w_1 - w_2}{w_1} \right) * 100 \qquad (1)$$

After that, a weight (W_1) of the powder was heated in an electrical furnace at 650°C for 3 h. The residual ash was cooled in a desiccator to obtain the final weight (W_2). The percent of ash was calculated by (Eq. 2):

$$Ash\% = \left(\frac{w_2}{w_1}\right)*100 \qquad (2)$$

Results from proximate and ultimate analysis of the lignocellulosic precursor are indicated in Table 1. It is obvious from the table that the relatively high amount of moisture belongs to the water absorbed on the starting material, and the relatively low amount of ash (4.5%) arises from the inorganic content. Because of ash content, this raw material has potential to be used as precursor for activated carbon production. Whereas, most high ash content in starting material is undesirable because it reduces the mechanical strength and adsorption capacity of activated carbon. On the other hand, the elemental analysis data showed that the raw material have a variation in the composition. It was observed that the steams of DH contain a large amount of oxygen and an important quantity of carbon. However, this material possesses a relatively low amount of hydrogen followed by nitrogen and sulfur content. Specifically, the highest amount of carbon content plays a significant role in the structure arrangement and aromatization.

2.2.2. Activated carbons preparation

The steams of the plant were crushed, sieved and the fraction with particle size of 1–2 mm was selected for the preparation of activated carbons. The powder was carbonized at 500 or 600°C in a tubular furnace during 2h and then impregnated with potassium hydroxide at KOH to carbon ratio (g KOH/ g carbon) of 1or 2 g/g. The mixture was shaken at 500 rpm in 100 ml of distilled water for 1h, and then kept at 110°C overnight to remove excess moisture. Further, the impregnated carbons were thermally activated at 400°C or 500°C during the desired activation time (1 or 2h).

The resulted activated carbons were washed with distilled water followed by 0.1 M hydrochloric acid solution and then washed by hot distilled water at 60°C to eliminate excess potassium. Finally, the samples were washed with deionized water until neutral pH. The obtained carbons were then dried at 105°C until constant weight, powdered using a domestic mixer and sieved in particles of size lower than 125 µm using a normalized sieve. The resulted powders were kept in hermetic bottles for further tests.

2.3. Characterization

2.3.1. Scanning electron microscopy (SEM)

The morphological characteristics of the optimal prepared activated carbons were analyzed by scanning electron microscopy using a FEI Quanta 200 model. Small amount of each sample was finely powdered and mounted directly onto aluminum sample holder using two-sided adhesive carbon model.

2.3.2. Iodine number (IN)

Iodine number is a widely used technique for rapid assessment of activated carbon quality. It is a measure of activation level (higher number indicates higher degree of activation). It is a measure of micropore content of the activated carbon (0–2 nm) by adsorption of iodine from solution. The iodine number was determined according to the ASTM D4607-94 method. 1g of each ACs are treated with 10.0 mL of 5% HCl and boiled for 30 s and subsequently cooled. 100 mL of 0.1 N iodine solution was added to the mixture and stirred for 30 min. The resulting solution was filtered and 50 mL of the filtrate was titrated with 0.1 N sodium thiosulfate using starch as indicator.

2.3.3. Methylene blue index (MB index)

The methylene blue index is a measure of mesoporosity (2–50 nm) present in activated carbon. It is defined as the maximum sorption capacity of methylene blue onto ACs. Stock solution of methylene blue was prepared by dissolving desired weight in distilled water. Sorption experiments were investigated in a series of beakers containing 100 mL by adding 100 mg of each ACs. Sorption equilibrium was established at room temperature for different methylene blue initial concentration between 20 and 500 mg/L. Then, in order to determine the residual concentration, the filtrate solutions were diluted and analyzed using TOMOS V-1100 UV-vis spectrophotometer at the maximum absorption wavelength of 665 nm.

2.3.3. Heavy metals removal

Solutions of cadmium and cobalt ions were prepared by dissolving desired weight of $Cd(NO_3)_2.4H_2O$ or $Co(NO_3)_2.6H_2O$ in distilled water. Sorption experiments were investigated in a series of beakers containing 50 mL of the metal ion solution at a concentration of 100 mg/L and 50 mg of each ACs. The mixtures were stirred for 3h at 500 rpm. The pH of the solutions was adjusted to 6.50 during the experiment with either 0.1M of HCl or NaOH and measured by a sensION+ PH31 pH meter.

After each sorption experiment, samples were centrifuged at 3400 rpm for 10 min and metal ions concentrations were determined using a PerkinElmer atomic absorption spectrophotometer (AAnalyst 200).

Table 1. Proximate and ultimate analysis of *Diplotaxis harra*

Precursor	Ultimate analysis (%)					Proximate analysis (%)	
	C	H	N	S	O	Moisture	Ash
DH	39.78	6.30	1.58	0.41	44.70	4.16	4.5

The adsorption capacity at equilibrium was defined as the amount of adsorbate per gram of adsorbent and was calculated using (Eq.3:

$$q_e = \frac{(c_0 - c)}{R} \qquad (3)$$

where q_e is the adsorbed quantity (mg/g), C_0 is the initial metal concentration (mg/L), C is the residual metal concentration (mg/L), and R is the mass of activated carbon per liter of aqueous solution (g/L).

Sorption equilibrium for the optimized activated carbons was established for different concentrations between 20 and 200 mg/L. The obtained data was correlated to Langmuir and Freundlich isotherm models via non-linear fitting using Origin 6.0 software.

2.4. Experimental design

Full factorial experimental design with two levels was used to investigate the significance of the effects of parameters on iodine number, MB index, cadmium and cobalt ions removal responses. Table 2 illustrates the ranges of the four factors used including, carbonization temperature (A), activation temperature (B), activation time (C) and impregnation ratio (D). These variables with their respective domain are chosen on the basis of the literature data and preliminary experiments.

Table 2. Process factors and their levels

Factors	Levels	
	Low (-)	High (+)
A. Carbonization temperature (°C)	500	600
B. Activation temperature (°C)	400	500
C. Activation time (h)	1.0	2.0
D. Impregnation ratio (g/g)	1.0	2.0

The experiments were performed to optimize the preparation conditions and to evaluate the metal ions removal. A first-order model with all possible interactions was chosen to fit the experimental data (Eq. 4). The main effects represent deviations of the average between the high and low levels for each factor. When the effect of a factor is positive, the response increases as the factor changes from low to high levels. In contrast, if the effects are negative, a reduction in response occurs for high level of the same factor (Cojocaru and Trznadel, 2007). The statistical experimental design and the observed data were generated and analyzed by Design Expert 8.0.7.1 Trial software.

The quality-of-fit of the model was checked by the coefficient of determination R^2 and R_{adj}^2. The R^2 value is a statistical measure of how well a model fits the real data points. R^2 values range from 0 to 1, where 1 represents the ideal model (Eq. 4).

$$Y = b_0 + b_1 A + b_2 B + b_3 C + b_4 D + b_{12} AB + b_{13} AC +$$
$$+ b_{14} AD + b_{23} BC + b_{24} BD + + b_{123} ABC + b_{124} ABD + \qquad (4)$$
$$+ b_{134} ACD + b_{234} BCD + b_{1234} ABCD$$

where, Y is the responses of interest (Iodine number (Y_1), methylene blue index (Y_2), adsorption capacity of Cd(II) (Y_3) and adsorption capacity of Co(II) (Y_4)).

3. Results and discussion

3.1. Experimental results

Table 3 gives the preparation conditions and the experimental results for the four responses; iodine number, methylene blue index, cadmium and cobalt ions removal. For iodine number, it appears that the carbonization temperature have a major effect on the response development during activation of the biomaterial. The higher iodine number of 696.84 mg/g is obtained for the carbon pyrolyzed at 500°C and activated at 500°C for 1 hour with an impregnation ratio of 1 g/g. For methylene blue index, it was seen that the activation temperature has the strong effect. The greater MB index of 235.64 mg/g was obtained for samples carbonized at 600°C, activated at 400°C during 1h with an impregnation ratio of 2 g/g. This result indicated a greater mesoporosity in studied field. For the Cd(II) removal, the maximum sorption capacity of 67.57 mg/g was obtained for the activated carbon prepared at carbonization temperature of 600°C and activated at 400°C with an impregnation ratio of 2 g/g during 1h. In the case of Co(II) removal, the highest capacity, 32.11 mg/g, was obtained for the activated carbon prepared at carbonization temperature of 600°C and activated at 500°C with an impregnation ratio of 2 g/g during 1h.

In fact, the regression analysis was performed to fit the response functions with the experimental data. Table 4 presents the values of regression coefficient obtained for individual factors and for the interaction between factors. Based on this table, it might be seen that the carbonization temperature present a negative effect on iodine number and a positive effect on the other responses. However, the activation temperature and the activation time have a positive effect on the iodine number and they present a negative impact on the remaining responses. Although, the impregnation ratio have a positive impact on the four responses.

Further, the analysis of the interaction effects shows a significant interaction between carbonization temperature and impregnation ratio on the iodine number (b_{14}= 22.87) with a positive impact, and a significant interaction between activation temperature and activation time on methylene blue index response with a positive effect (b_{23}= 21.35). For the heavy metal ions removal, the interaction between carbonization temperature, activation temperature and impregnation ratio was the most significant with a positive sign (b_{124}=3.84 for cadmium and b_{124}= 2.81 for cobalt).

3.2. Analysis of variance (ANOVA)

To determine the most important main and interaction effects of the curvature in the responses, analysis of variance (ANOVA) was done at a confidence level of 95%. After discarding the

insignificant terms, the ANOVA data for the coded quadratic models are presented in Tables 5–8.

The ANOVA results showed that the equations adequately represented the actual relationship between each response and the significant variables. The F-value implies that the models are significant and values of "Prob> F" less than 0.05 in the ANOVA table. F-test was used to estimate the statistical significance of all terms in the polynomial equation within 95% confidence interval. Subsequently, larger F-value with the associated P value (smaller than 0.05, confidence interval) means that the experimental systems can be modeled effectively with less error. Then, for modeling the experimental system, the interaction effects as significant model terms can be used.

3.2.1. Iodine number

According to the ANOVA analysis for the iodine number, the main significant effects are carbonization temperature (A), activation temperature (B), and the interaction effects; AC and AD (Eq. 5).

$$Y1 = 581.47 - 34.72A + 32.10B + 19.37AC + 22.87AD \quad (5)$$

The carbonization temperature showed a negative impact on the iodine number. While, activation temperature, interaction between carbonization and activation time, and the interaction between carbonization temperature and impregnation ratio have a positive effect. In fact, the increasing of carbonization temperature reduces the iodine number. Whereas, the increase of activation temperature, the interaction between carbonization temperature and activation time and also, the interaction between carbonization temperature and impregnation ratio allows the increasing of the iodine number which increase the microporosity of activated carbons.

3.2.2. Methylene blue index

For the methylene blue index, the most significant effects are activation temperature (B), impregnation ratio (D) and the interaction between activation temperature and activation time (BC) (Eq. 6).

Table 3. Factorial experimental design matrix coded, real values and experimental results for each response

Run	Coded values				Actual values				Responses (mg/g)			
	A	B	C	D	A	B	C	D	IN	MB index	Cd(II)	Co(II)
1	-1	-1	-1	-1	500	400	1	1.00	627.03	109.31	40.85	16.06
2	+1	-1	-1	-1	600	400	1	1.00	487.41	114.89	50.39	25.01
3	-1	+1	-1	-1	500	500	1	1.00	696.84	28.99	15.66	3.40
4	+1	+1	-1	-1	600	500	1	1.00	501.37	46.54	14.13	2.79
5	-1	-1	+1	-1	500	400	2	1.00	571.18	74.73	36.27	13.90
6	+1	-1	+1	-1	600	400	2	1.00	515.33	103.19	41.61	14.51
7	-1	+1	+1	-1	500	500	2	1.00	613.07	122.61	11.08	1.55
8	+1	+1	+1	-1	600	500	2	1.00	543.26	50.27	9.17	1.24
9	-1	-1	-1	+1	500	400	1	2.00	557.22	207.71	67.19	31.49
10	+1	-1	-1	+1	600	400	1	2.00	508.35	235.64	67.57	29.95
11	-1	+1	-1	+1	500	500	1	2.00	654.85	108.52	16.42	2.48
12	+1	+1	-1	+1	600	500	1	2.00	606.09	65.43	62.22	32.11
13	-1	-1	+1	+1	500	400	2	2.00	599.1	108.24	50.01	20.38
14	+1	-1	+1	+1	600	400	2	2.00	529.29	172.61	58.79	24.08
15	-1	+1	+1	+1	500	500	2	2.00	610.27	52.39	35.51	11.12
16	+1	+1	+1	+1	600	500	2	2.00	682.88	157.18	41.99	18.22

Table 4. Values of model coefficients for the four responses

Main coefficients	Y1	Y2	Y3	Y4
b_0	581.47	109.89	38.67	15.51
b_1	-34.72	8.32	4.55	2.97
b_2	32.10	-30.90	-12.90	-6.40
b_3	1.57	-4.73	-3.12	-2.39
b_4	12.03	28.57	11.28	5.70
b_{12}	4.54	-7.46	1.55	1.50
b_{13}	19.36	7.33	-2.21	-1.58
b_{14}	22.87	10.92	3.12	1.89
b_{23}	-2.785	21.35	1.78	1.31
b_{24}	12.90	-11.68	1.98	1.15
b_{34}	10.30	-11.12	-0.26	-0.38
b_{123}	11.51	-0.08	-2.74	-1.19
b_{124}	13.27	3.63	3.84	2.81
b_{134}	-6.81	15.70	-1.64	-0.57
b_{234}	-1.04	3.40	1.31	0.15
b_{1234}	6.27	14.01	-3.22	-2.27

Table 5. Analysis of variance for iodine number

Source	Sum of Squares	df	Mean Square	F Value	p-value Prob> F	
Model	50155.50	4	12538.87	10.21	< 0.0011	significant
A	19291.82	1	19291.82	15.71	< 0.0022	
B	16494.26	1	16494.26	13.43	0.0037	
AC	6000.82	1	6000.82	4.88	0.0491	
AD	8368.59	1	8368.59	6.81	0.0242	
Residual	13505.05	11	1227.73			
Cor Total	63660.55	15				

$R^2 = 0.7878; R_{adj}^2 = 0.7107$

Table 6. Analysis of variance for methylene blue index

Source	Sum of Squares	df	Mean Square	F Value	p-value Prob> F	
Model	35640.75	3	11880.25	8.49	0.0027	significant
B	15277.47	1	15277.77	10.92	0.0063	
D	13063.77	1	13063.77	9.34	0.0100	
BC	7299.51	1	7299.51	5.22	0.0413	
Residual	16779.18	12	1398.26			
Cor Total	52419.94	15				

$R^2 = 0.6799; R_{adj}^2 = 0.5998$

Table 7. Analysis of variance for cadmium ion removal

Source	Sum of Squares	df	Mean Square	F Value	p-value Prob> F	
Model	4701.88	2	2350.94	20.78	<0.0007	significant
B	2664.84	1	2664.84	23.56	0.0003	
D	2037.04	1	2037.04	18.01	0.0010	
Residual	1470.16	13	5.53			
Cor Total	6172.05	15				

$R^2 = 0.7618; R_{adj}^2 = 0.7251$

Table 8. Analysis of variance for cobalt ion removal

Source	Sum of Squares	df	Mean Square	F Value	p-value Prob> F	
Model	1177.88	2	588.94	11.67	0.0013	significant
B	656.24	1	656.24	13.005	0.0032	
D	521.64	1	521.64	10.33	0.0068	
Residual	655.95	13	50.45			
Cor Total	1833.84	15				

$R^2 = 0.6423; R_{adj}^2 = 0.5872$

$$Y2 = 109.89 - 30.90B + 28.57D + 21.36BC \qquad (6)$$

The activation temperature has a negative effect on the methylene blue index response. Although, activation time and the interaction between activation temperature and activation time present a positive effect. Thus, the methylene blue index increases when impregnation ratio and the interaction between activation temperature and activation time increase. However, if the activation temperature increases a reduction of mesopores is observed. Therefore, to increase the methylene blue index, we shall operate under low activation temperature (400°C).

3.2.3. Heavy metals removal

According to the ANOVA data for the Cd(II) and Co(II) responses, the most significant factors are activation temperature (B) and impregnation ratio (D) (Eqs. 7-8), Table 7 and 8.

$$Y3 = 38.68 - 12.91B + 11.28D \qquad (7)$$

$$Y4 = 15.52 - 6.40B + 5.71D \qquad (8)$$

The activation temperature presented a negative impact on cadmium and cobalt ions removal. However, impregnation ratio has a positive effect. Indeed, the removal of heavy metals decreased when the activation temperature increases and increases if the impregnation ratio increases. Then, the interactions between factors are not significant as their corresponding P values are > 0.05. Hence, it could be seen that the models for cadmium and cobalt removal are similar. The both models are correlated to the methylene blue index model. This result indicates that

the cadmium and cobalt ions were adsorbed in mesopores. Moreover, the decrease in the number of mesopores is accompanied by a significant reduction of the adsorption capacity of both heavy metals onto activated carbon samples.

3.3. Diagnostic model

Experimental and predicted values for each response are presented in Table 6. It can be observed the small difference between the experimental and predicted response which indicates the adequacy of the models. The correlation between the theoretical and experimental responses, calculated by the model, is satisfactory. Therefore, the "R^2" are in reasonable agreement with the "R_{Adj}^2". It can be seen that, more than 95% of the four responses can be well predicted by the models, indicating that the terms which were considered in the proposed models are significant enough to make acceptable predictions.

However, adding more terms improve the model adequacy. For the iodine number, methylene blue index, cadmium and cobalt removal, the Model F-values of 10.21, 8.50, 20.79 and 11.67, respectively, implies that models are significant. There are only a 0.11%, 0.27%, 0.01% and 0.13%, chance for the iodine number, MB index, cadmium and cobalt removal respectively. Hence, the large value of F confirms the adequacy of model fits.

3.4. Response surface analysis

In the next step of the design, response surface methodology (RSM) was developed by considering the significant interactions in the full experimental design to optimize the critical factors and describe the nature of the response surface in the experiment. Fig.1 and Fig.2 present the 3D response surfaces plots for the significant interactions for iodine number and methylene blue index respectively. For the iodine

number, the most significant interactions were the activation time/carbonization temperature and the impregnation ratio/activation temperature. While, the best significant interaction for methylene blue index was the combination between activation time and activation temperature. In the removal of cadmium and cobalt, there are no significant interactions between the individual factors.

For iodine number, it could be seen from Fig.1a that the iodine number increased with increasing activation time and decreasing carbonization temperature, when activation temperature is fixed at 500°C and impregnation ratio at 1 g/g. Maximal iodine number was observed at a carbonization temperature of 500°C regardless the activation time. Fig.1b indicates that at lower carbonization temperature regardless the impregnation ratio, the iodine number increases. Therefore, a maximal iodine number is obtained at carbonization temperature of 500°C with impregnation ratio of 2 g/g and when the activation temperature is fixed at 500°C during 1 hour.

On the other hand, the Fig.2 shows that the MB index increased at lower activation temperature whatever the activation time, if the carbonization temperature is fixed at 600°C and impregnation ratio at 2 g/g. The higher MB index was obtained at activation temperature of 400°C regardless the activation time, which clearly indicate that the mesoporosity of activated carbon depend on the combination between activation temperature and activation time.

3.5. Normal probability plot of residuals

A normal probability plot of the residuals may be audit the normal probability of calculate data. When, the data points on the plot fall fairly close to the straight line, then the data are normally distributed (Gratuito et al., 2008). The normal probability plot of the residuals for ACs was shown in Fig. 3.

Table 6. Factorial design matrix of four variables along with experimental and predicted responses for IN, MB index, Cd(II) and Co(II)

| Run	IN			MB index			Cd(II)			Co(II)		
	Actual	*Predicted*	*Residual*	*Actual*	*Predicted*	*Residual*	*Actual*	*Predicted*	*Residual*	*Actual*	*Predicted*	*Residual*
1	654.85	644.80	10.05	108.52	86.21	22.31	16.42	37.06	-20.63	2.48	14.82	-12.35
2	613.07	651.81	-38.74	122.61	71.78	50.83	11.08	14.49	-3.41	1.55	3.40	-1.85
3	557.22	580.58	-23.36	207.71	190.72	16.99	67.19	62.87	4.32	31.49	27.63	3.86
4	606.09	582.36	23.73	65.43	86.21	-20.78	62.22	37.06	25.17	32.11	14.82	17.28
5	571.18	587.59	-16.41	74.73	90.86	-16.12	36.27	40.30	-4.03	13.90	16.21	-2.31
6	610.27	606.07	4.20	52.39	128.92	-76.53	35.51	37.06	-1.55	11.12	14.82	-3.70
7	508.35	518.14	-9.79	235.64	190.72	44.91	67.57	62.87	4.70	29.95	27.63	2.31
8	515.33	511.14	4.19	103.19	90.86	12.33	41.61	40.30	1.31	14.51	16.21	-1.70
9	501.37	536.62	-35.25	46.54	29.06	17.49	14.13	14.49	-0.36	2.79	3.40	-0.62
10	599.1	541.85	57.25	108.24	148.01	-39.76	50.01	62.87	-12.86	20.38	27.63	-7.25
11	682.88	621.09	61.79	157.18	128.92	28.26	41.99	37.06	4.94	18.22	14.82	3.40
12	696.84	690.54	6.30	28.99	29.06	-0.07	15.66	14.49	1.17	3.40	3.40	0.00
13	627.03	626.32	0.71	109.31	133.58	-24.27	40.85	40.30	0.55	16.06	16.21	-0.15
14	487.41	472.40	15.01	114.89	133.58	-18.68	50.39	40.30	10.09	25.01	16.21	8.80
15	529.29	556.88	-27.59	172.61	148.01	24.60	58.79	62.87	-4.08	24.08	27.63	-3.55
16	543.26	575.35	-32.09	50.27	71.78	-21.51	9.17	14.49	-5.32	1.24	3.40	-2.16
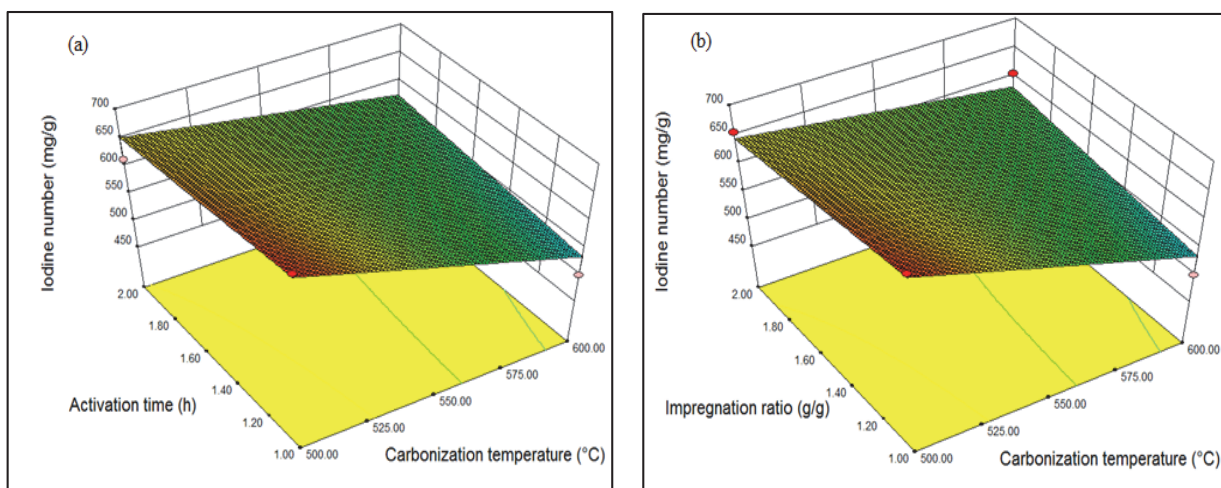
Fig. 1. Surface response plot for the iodine number
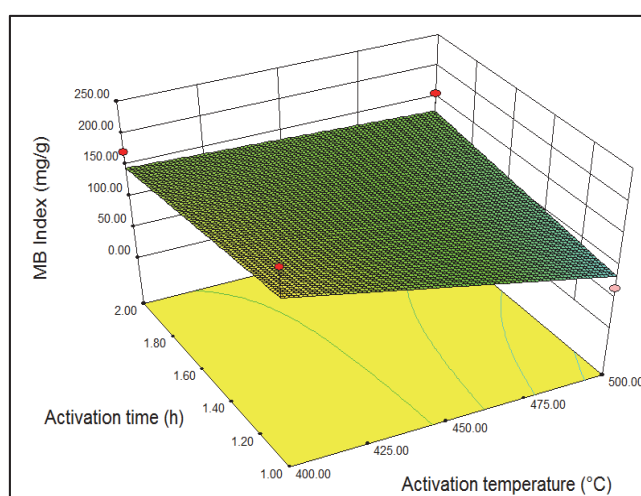

Fig. 2. Surface response plot for the MB index

From Fig. 3 it's appears that for each response, the data points were fairly close to the straight line and it indicates that the experiments come from a normally distributed population.

3.6. Optimization

The four responses were optimized simultaneously by using the desirability function approach. This function approach is a popular and established technique for the simultaneous determination of optimum settings of input variables that can determine optimum performance levels for one or more responses. Harrington (1965) first developed the desirability function, and it was later modified by Derringer and Suich (1980) for specifying the relationship between predicted responses on a dependent variable and the desirability of the responses. All variables were considered equally important, and thus the weights for the response variables were set to one. The maximum value of the desirability function (1.000) was obtained at a carbonization temperature of 600°C, an activation temperature of 400°C, an activation time of 2h, and an impregnation ratio of 1 g/g. At these conditions, the predicted responses for the iodine number, methylene blue index, Cd(II) and Co(II) were 511.13 ± 35.03 mg/g, 90.85 ± 37.39 mg/g, 40.30 ± 10.63 mg/g and 16.21 ± 7.10 mg/g, respectively. To validate the predicted responses, experiments were conducted at the optimal conditions, obtaining a maximal values.
In fact, the maximum iodine number and methylene blue index were 780.61 mg/g and 161.92 mg/g respectively. Moreover, the best sorption of cadmium and cobalt were 57.87 mg/g and 45.75 mg/g, respectively. The validity of experiments at the optimized value of all parameters closely correlated with the desirability optimization analysis using full factorial experimental was observed.

3.7. Morphology of ACs

The SEM photographs for ACs samples activated in different conditions are exhibited in Fig.4. The images showed that the ACs has morphology with a well-developed porous structure. Therefore, the

external surface of the ACs contains crevices, cracks, and some grains and pores in various sizes in large holes. In fact and after activation, more porous structures begin to appear which can be attributed to the dehydration effect of KOH and the oxidation of organic compounds in the carbonization step. In Fig. 4a-d, the samples exhibit an identical morphology that is characterized by a smooth surface with many orderly pores developed and regular shaped and macropores with wide net nested cavities.

While, the activated carbons prepared at carbonization temperature of 600°C, activation temperature of 500° during 1h with an impregnation ratio of 2 g/g (Fig. 4e) and the other one prepared at carbonization temperature of 600°C, activation temperature of 400°C at 1h with an impregnation ratio in order of 2 g/g (Fig. 4f) present an external surface plenty of channels contain holes and wrinkles of different sizes. This result can be due to the lack impurities such as tar that could clog up the pores and inhibit good pore structure development. Whereas, these samples present an efficient sorption of cadmium and cobalt. Hence, we can say that the large porosity does not imply a greater sorption. Therefore, the difference observed in Acs surfaces can be attributed to the preparation conditions in the process activation.

Char usually contains 75-80% carbon; some oxygen, (15-17%) and some hydrogen, (<3%) (Collins et al., 2006). Tars consists of phenols, CH_3COOH,

CH_3OH, $(CH_3)_2CO$, and other high molecular weight hydrocarbons. The gaseous components include among others H_2O, CO_2, CO. The following reaction occurred during the activation (second stage) process (Collins et al., 2006).

$$C + 2KOH \rightarrow 2K + H_2 + CO_2$$

$$C + 2KOH \rightarrow 2K + H_2O + CO$$

$$CO_2 + 2KOH \rightarrow K_2CO_3 + H_2O$$
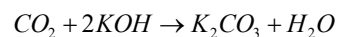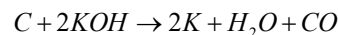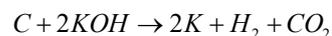
Potassium intercalated with the carbon matrix during activation, resulting in the widening and formation of new pores (Collins et al., 2006).

$$H_2O + C + 2KOH \rightarrow K_2CO_3 + 2H_2$$

The effect of change in carbonization temperature, activation temperature, activation time and impregnation ratio were most significantly influencing the porous characteristics which influencing the cadmium and cobalt ions removal. The iodine number decreased as the carbonization temperature increased from 500 to 600°C. This is because the increase of temperature of pyrolysis resulted more volatile component being lost, which caused a destruction of micropores, and hence a decreasing of microporosity of the activated carbon samples at 600°C which are confirmed by the result observed in SEM images.
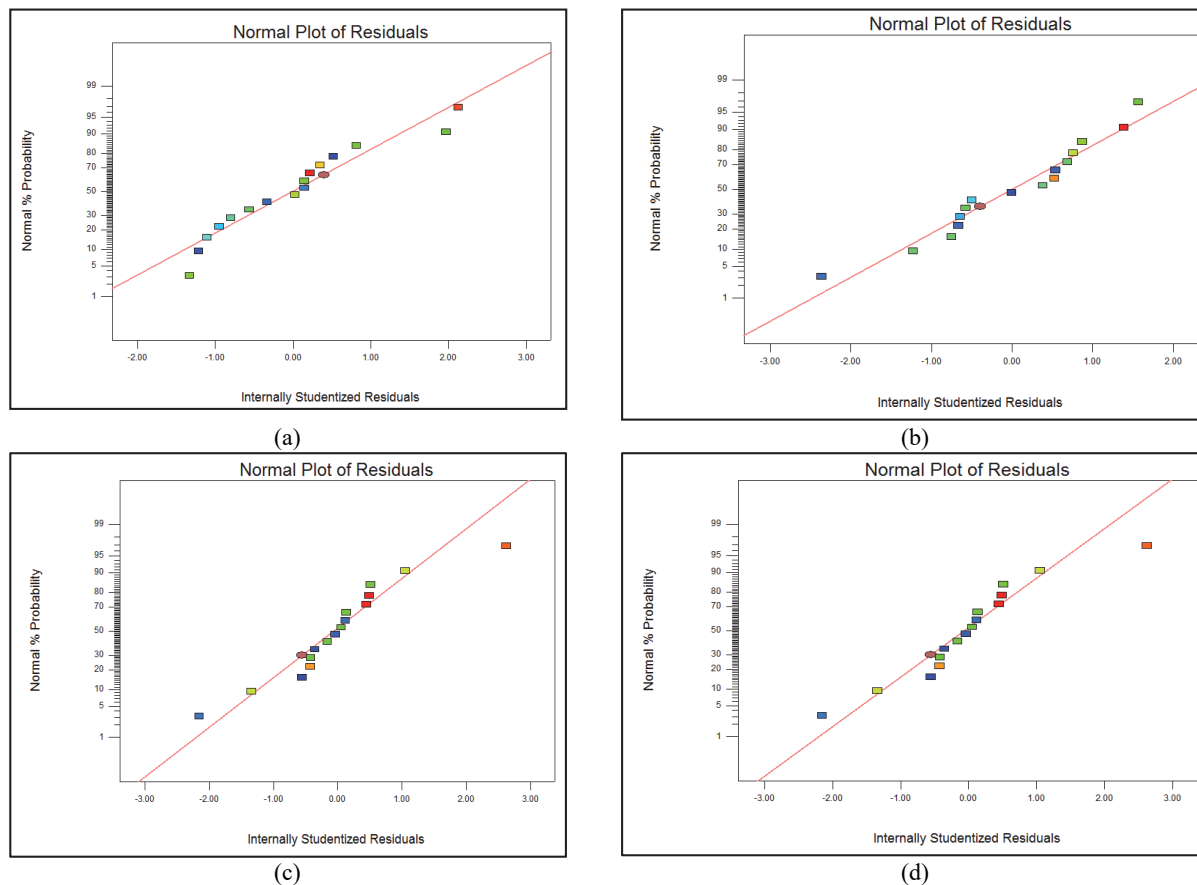

(a) (b) (c) (d)

Fig. 3. Normal probability plots of residuals for the four responses: (a) Iodine number, (b) MB index, (c) Cd(II) and (d) Co(II) removal capacities
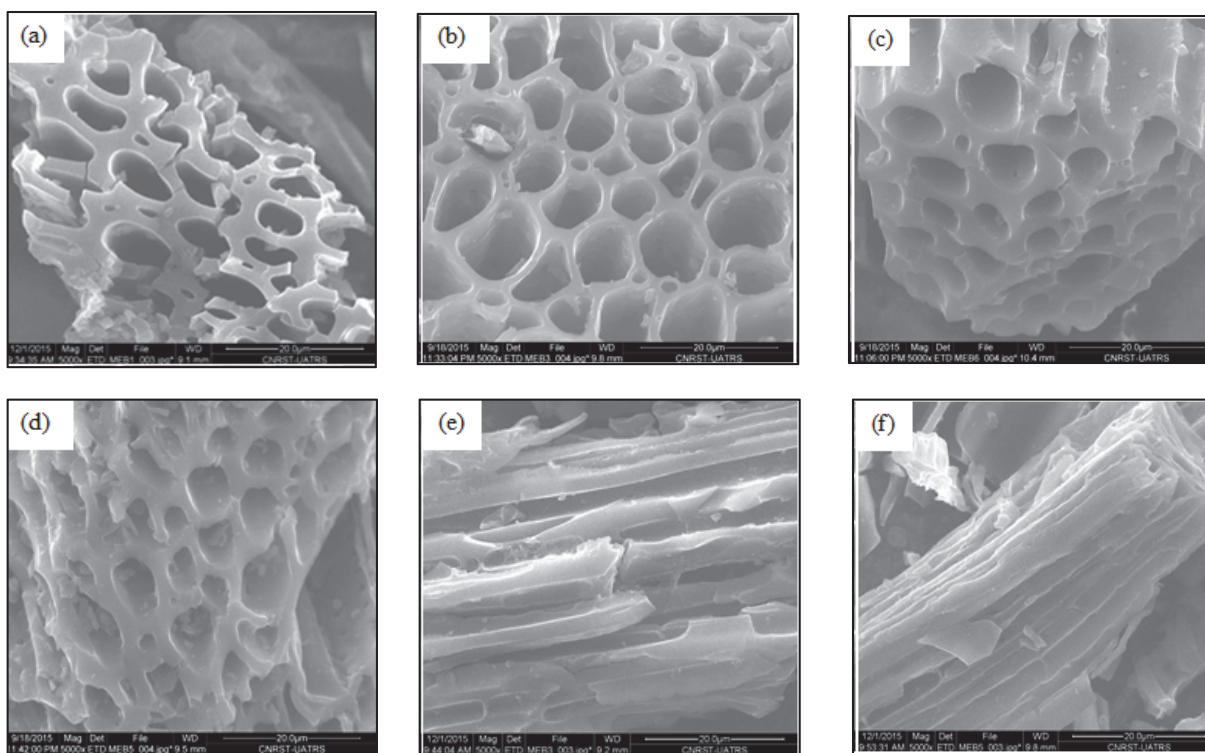
Fig. 4. SEM micrographs of Acs- : (a) 500°C/ 400°C/ 1h/ 2(g/g); (b) 500°C/ 500°C/ 1h/ 1(g/g); (c) 500°C/ 500°C/ 2h/ 1(g/g); (d) 500°C/ 400°C/ 2h/ 2(g/g); (e) 600°C/ 500°C/ 1h/ 2(g/g) and (f) 600°C/ 400°C/ 1h/ 2(g/g)

It is also clear that the influence of activation time was more pronounced at higher temperatures. Although, the MB index decreases with the increasing of activation temperature from 400 to 500°C. The effect of activation temperature and time is moreover most significant at the highest carbonization temperature of 600°C. It has also been reported that increasing of the impregnation ratio at 2 g/g increases the MB index. This is because the potassium ions fixed onto the carbon surface proceed as catalyst to accelerate the reaction between the carbon and KOH. Therefore, the influence of time is much less significant than that of temperature on the preparation conditions of ACs. In fact, the sorption of cadmium and cobalt are more influenced by activation temperature and impregnation ratio. The removal of the both heavy metals increased as the impregnation ratio increased from 1 to 2 g/g. Further, it was observed a reduction of the adsorption capacities of Cd(II) and Co(II), when the activation temperature increased from 400°C to 500°C. Thus, it could be seen that the both heavy metals influenced by the same as factors that influence the MB Index, which contribute that the modal of the cadmium and cobalt was similar to those of MB Index. Hence, the both heavy metals can sorbed on mesopores.

On the other hand, the characteristics of the commercial activated carbon, which are further determined were 1115.7 mg/g for iodine number and 288.9 mg/g for methylene blue index, 0.8 mg/g for cadmium removal and 21.2 mg/g for cobalt removal. Thus, the high sorption efficiencies of ACs were shown greater than those of commercial activated carbon. However, the commercial activated carbon had a high microporosity and mesoporosity in comparison with those greater of ACs.

3.9. Sorption isotherm modeling

The use of experimental design has allowed the optimization of the preparation conditions and the evaluation of heavy metals removal onto prepared activated carbons. Hence, the activated carbons having a highest potential ability to remove heavy metal ions were established. Indeed, the activated carbon that is carbonized at 600°C, activated at 500°C during 1h with an impregnation ratio of 2g/g and the activated carbon carbonized at 600°C, activated at 500°C during 1h with an impregnation ratio of 2g/g were considered as optimized activated carbons for studding the isotherm models of cadmium and cobalt ions sorption respectively. The sorption isotherms were reported inFig.5, and the different parameters obtained after modeling isotherms were tabulated in Table 7. From the Fig. 5, it can be seen that the sorption efficiency increases upon increasing of initial concentration, indicating that the sorption process is more favorable at increasing concentration of metal ions. In fact, the AC carbonized at 600°C, activated at 400°C during 1h with an impregnation ratio of 2g/g has a greater sorption efficiency of cadmium and the AC carbonized at 600°C, activated at 500°C during 1h with an impregnation ratio of 2g/g has high sorption of cobalt ion. This result may be related to the external morphology of each activated carbon. When, the both activated carbons present an external surface plenty of channels contain holes and wrinkles of different sizes with a mesopores in the ends of channels. Whereas,

the activated carbons with a large porosity not show a large porosity. Furthermore, the ANOVA analysis indicated that the sorption of Cd(II) and Co(II) can be done in mesopores (the model of heavy metals is suitable with the model of MB index). Then, the mesoporosity occurs her greater value at the optimized conditions of AC carbonized at 600°C, activated at 400°C during 1h with an impregnation ratio of 2g/g, that present a highest sorption efficiency of Cd(II). However, the optimized conditions of AC carbonized at 600°C, activated at 400°C during 1h with an impregnation ratio of 2g/g, present a fewer mesopority. This, this activated carbon has a most sorption capacity of Co(II) ions. The equilibrium characteristics were described through Langmuir and Freundlich isotherm models.

Langmuir isotherm model is one of the most popular isotherms using for the removal of heavy metals by activated carbons to evaluate the maximum sorption capacity of a sorbate on a sorbent. It assumes that sorption occurs onto monolayer coverage of sorbate over a homogenous sorbent surface (Langmuir, 1916). This model supposes that sorption occurs on specific homogeneous sites within the sorbent and all its sorption sites are energetically identical. The Langmuir isotherm can be given as (Eq. 9):

$$q_e = \frac{q_m K_L C_e}{1 + K_L C_e}$$
(9)

where q_m (mg/g) is the maximum monolayer sorption capacity, K_L(L/mg) is the Langmuir equilibrium constant related to the sorption affinity and C_e is the equilibrium concentration.

The Freundlich model assumes heterogeneous surface energy. This model is widely used to describe adsorption with non-uniform distribution of the heat of sorption and affinities (Freundlich and Heller, 1939). The no-linear form of the Freundlich can be stated as follows (Eq. 10):

$$q_e = K_F C_e^{1/n}$$
(10)

where K_F (mg$^{1-1/n}$/ g/ Ln) and n are Freundlich constants. n is the heterogeneity factor related to sorption affinity and K_F is related to the sorption capacity. In general, if the values of n are in the range of 1–10, it can be considered that the extraction process indicates that adsorbate is favorably adsorbed on the adsorbent. However, the sorption is very insignificant when n is lower than 1. Also, if the value of n is equal to unity, the adsorption is linear; if the value is below to unity, it can be deduced that adsorption process is chemical, if the value is above unity adsorption is a favorable physical process.

According the results listed in Table 5, the correlation coefficients of the both isotherms of the cadmium and cobalt sorption were always higher. While, the Langmuir isotherm model ($r^2 = 0.99$) appeared to be much more applicable than the Freundlich. The fitness of the Langmuir model to the adsorption process assumes that the Cd(II) and Co(II) ions were adsorbed on specific monolayer onto activated carbons. Although, the results from the Freundlich show that the n is greater than unity, which further supports the favorable sorption of Cd(II) and Co(II) onto the both optimized activated carbons.

Therefore, the maximum sorption capacities obtained with the application of the Langmuir isotherm model are 118.09 for cadmium sorption and 48.89 mg/g for cobalt sorption onto AC carbonized at 600°C, activated at 400°C during 1h with an impregnation ratio of 2g/g and AC carbonized at 600°C, activated at 500°C during 1h with an impregnation ratio of 2g/g respectively. For cadmium and cobalt ions sorption, the sorption processes are done in homogenous sites with sorption capacities close to those experimental sorption capacities at equilibrium.
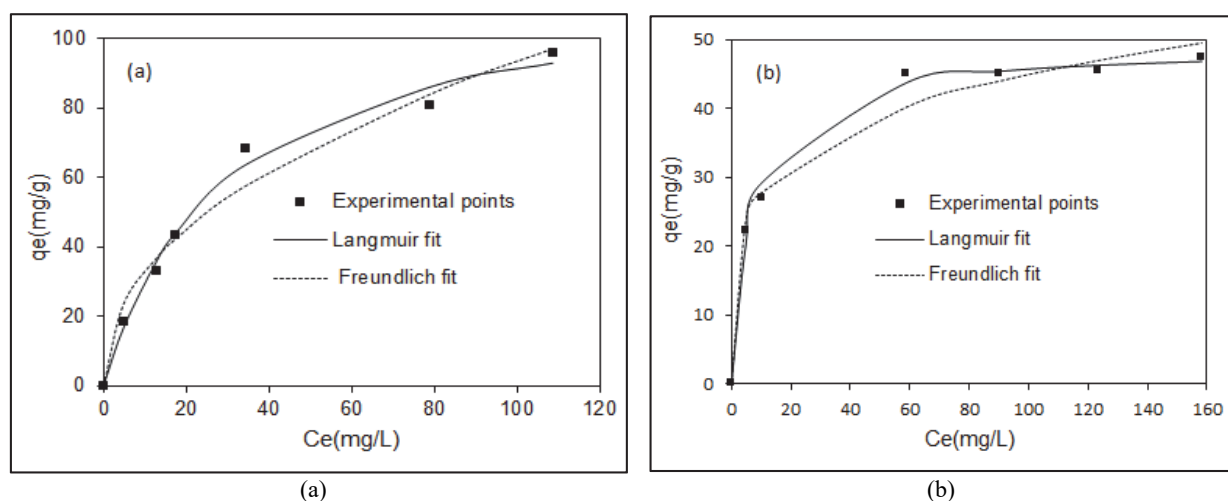

(a)

(b)

Fig. 5. Experimental points and nonlinear fitted curves isotherms: (a) Cd(II) onto 600/400/1h/2g/g, (b) Co(II) onto 600/500/1h/2g/g

Table 7. Isotherm parameters for the sorption of Cd(II)) onto 600/400/1h/2g/g and Co(II) onto 600/500/1h/2g/g

Isotherm model	Parameters	AC- 600/400/1h/2g/g	AC- 600/500/1h/2g/g
		Cd(II)	Co(II)
Langmuir	q_m (mg/g)	118.09	48.89
	K_L (L/mg)	0.03	0.14
	r^2	0.99	0.99
Freundlich	n	2.20	4.74
	K_F (mg$^{1-1/n}$ /g/L^n)	11.53	17.02
	r^2	0.97	0.98

4. Conclusions

Based on the above presented results, safely we may conclude that the *Diplotaxis harra* can be used as efficient precursor for the production of activated carbons. It was observed that the potassium hydroxide is a fast and sensitive chemical agent in process activation for better removal of heavy metals from aqueous solutions.

Analysis of different effects of factors (Carbonization temperature, activation temperature, activation time and impregnation ratio) indicates that the most influential factor on the iodine number is the carbonization temperature with a negative effect. Whereas, activation temperature has a strong impact with negative impact on methylene blue index. Therefore, the removal of cadmium and cobalt responses were negatively influenced by activation temperature and positively influenced by impregnation ratio.

The optimal conditions for greater amount of iodine number were obtained at carbonization temperature of 500°C, activation temperature of 500°C, activation time of 1h with impregnation ratio of 1 g/g. For methylene blue index the high value is occurred at carbonization temperature of 600°C, activation temperature of 400°C, activation time of 1h with impregnation ratio of 2 g/g. Furthermore, the best removal of cadmium was obtained also at a carbonization temperature of 600°C with an activation temperature of 400°C in one hour with an impregnation ratio of 2 g/g.

Hence, the efficient removal of cobalt is indicated at a carbonization temperature of 600°C with an activation temperature of 500°C in one hour with an impregnation ratio of 2 g/g. At these optimal conditions, the maximum iodine number and methylene blue index were 696.84 mg/g and 235.64 mg/g respectively. Moreover, the best sorption efficiencies of cadmium and cobalt ions were 67.57 mg/g and 32.11 mg/g respectively. These sorption efficiencies were shown greater than those of commercial activated carbon which are 0.85 mg/g for cadmium and 21.24 mg/g for cobalt removal. Subsequently, the maximum sorption capacities obtained with the application of the Langmuir isotherm model are 118.09 for cadmium sorption onto AC carbonized at 600°C, activated at 400°C during 1h with an impregnation ratio of 2g/g and 48.89 mg/g for cobalt sorption onto and AC carbonized at 600°C, activated at 500°C during 1h with an impregnation ratio of 2g/g respectively.

References

Ab Razak N.H., Praveena S.M., Aris A.Z., Hashim Z., (2015), Drinking water studies: A review on heavy metal, application of biomarker and health risk assessment (a special focus in Malaysia), *Journal of Epidemiology and Global Health*, **5**, 297– 310.

Ali Fil B., Erdem Yilmaz A., Boncukcuoğlu R., Bayar S., (2018), Kinetics and isotherm analysis of Cd²⁺ removal from aqueous solutions by ion exchange process, *Environmental Engineering and Management Journal*, **17**, 1967-1976.

Barka N., Ouzaouit K., Qourzal S., Assabbane A., Abdennouri M., El Makhfouk M., Nounah A., Ait-Ichou Y., (2012). Kinetics and equilibrium of cadmium removal from aqueous solutions by sorption onto synthesized hydroxyapatite, *Desalination and Water Treatment*, **43**, 8–16.

Carrillo-Chavez A., Salas-Megchun E., Levresse G., Muñoz-Torres C., Pérez-Arvizu O., Gerke T., (2014), Geochemistry and mineralogy of mine-waste material from a "skarn-type" deposit in central Mexico: Modeling geochemical controls of metals in the surface environment, *Journal of Geochemical Exploration*, **144**, 28–36.

Chayid M.A., Ahmed M.J., (2015), Amoxicillin adsorption on microwave prepared activated carbon from 2 Arundodonax Linn: Isotherms, kinetics, and thermodynamics studies, *Journal of Environmental and Chemical Engineering*, **3**, 1592–1601.

Cojocaru C., Trznadel G.Z., (2007), Response surface modeling and optimization of copper removal from aqua solutions using polymer assisted ultrafiltration, *Journal of Membrane Sciences*, **298**, 56–70.

Collins J.C., Zain M.F.H., Dek F.S., (2006), Treatment of landfill leachate in Kayumadang, sabah: textural and physical characterization (Part I). *Malaysian Journal of Analytical Sciences*, **10**, 1–6.

Derringer G., Suich R., (1980), Simultaneous optimization of several response variables, *Journal of Quality and Technology*, **12**, 214–219.

Ebbers B., Ottosen L.M., Jenssen P.E., (2015), Electrodialytic treatment of municipal wastewater and sludge for the removal of heavy metals and recovery of phosphorus, *Electrochemical Acta*, **181**, 90–99.

Freundlich H., Heller W., (1939), The adsorption of cis- and trans-azobenzene, *Journal of American Chemical Society*, **61**, 2228–2230.

Gao Y., Yue Q., Gao B., (2015), Insights into properties of activated carbons prepared from different raw precursors by pyrophosphoric acid activation, *Journal of Environmental Sciences*, **41**, 235-243.

Georgina J., Dottob G.L., Mazuttib M.A., Foletto E.L., (2016), Preparation of activated carbon from peanut shell by conventional pyrolysis and microwave irradiation-pyrolysis to remove organic dyes from

aqueous solutions, *Journal of Environmental and Chemical Engineering*, **4**, 266-275.

Gratuito M.K.B., Panyathanmaporn T., Chumnanklang R.A., Sirinuntawittaya N.B., Dutta A., (2008), Production of activated carbon from coconut shell: Optimization using response surface methodology, *Bioresource Technology*, **99**, 4887-4895.

Gundogdu A., Duran C., Senturk H.B., Soylak M., Ozdes D., Serencam H., Imamoglu M., (2012), Adsorption of phenol from aqueous solution on a low-cost activated carbon produced from tea industry waste: equilibrium, kinetic, and thermodynamic study, *Journal of Chemical and Engineering Data*, **57**, 2733-2743.

Gundogdu A., Duran C., Senturk H.B., Soylak M., Onal M.I.Y., (2013), Physicochemical characteristics of a novel activated carbon produced from tea industry waste, *Journal of Analytical and Applied Pyrolysis*, **104**, 249-259.

Guoa Z., Fanb J., Zhanga J., Kanga Y., Liua H., Jianga L., Zhanga C., (2015), Sorption heavy metal ions by activated carbons with well-developed microporosity and amino groups derived from *Phragmites australis* by ammonium phosphates activation, *Journal of the Taiwan Institute of Chemical Engineers*, **58**, 290–296.

Harrington E.C., (1965), The desirability function, *Industrial Quality Control*, **21**, 494-498.

Jung S.H., Kim J.S., (2014), Production of biochars by intermediate pyrolysis and activated carbons from oak by three activation methods using CO_2, *Journal of Analytical and Applied Pyrolysis*, **107**, 116-122.

Kilpima S., Runtti H., Kangas T., Lassi U., Kuokkanen T., (2014), Physical activation of carbon residue from biomass gasification: Novel 2 sorbent for the removal of phosphates and nitrates from aqueous 3 solutions, *Journal of Industrial and Engineering Chemistry*, **21**, 1354-1364.

Kima B., Gautier M., Prost-Bouclec S., Mollec P., Michel P., Gourdon R., (2014), Performance evaluation of partially saturated vertical-flow constructed wetland with trickling filter and chemical precipitation for domestic and winery wastewaters treatment, *Ecological Engineering*, **71**, 41-47.

Langmuir I., (1916), The constitution and fundamental properties of solids and liquids, *Journal of the American Chemical Society*, **38**, 2221-2295.

Li W., Tan S., Shi Y., Li S., (2015), Utilization of sargassum based activated carbon as a potential waste derived catalyst for low temperature selective catalytic reduction of nitric oxides, *Fuel*, **160**, 35-42.

Liu D., Zhang W., Lin H., Li Y., Lu H., Wang, Y., (2016), A green technology for the preparation of high capacitance rice husk-based activated carbon, *Journal of Cleaner Production*, **112**, 1190–1198.

Lofrano G., Carotenuto M., Libralato G., Domingos R.F., Markus A., Dini L., Gautam R.K., Baldantoni D., Rossi M., Sharma S.K., Chandra Chattopadhyaya M., Giugni M., Meric S., (2016), Polymer functionalized nanocomposites for metals removal from water and wastewater: an overview, *Water Research*, **92**, 22 –37.

Mahamad M.N., Zaini M.A.A., Zakaria Z.A., (2015), Preparation and characterization of activated carbon from pineapple waste biomass for dye removal, *International Biodeterioration & Biodegradation*, **102**, 274–280.

Njokua V.O., Islama M.A., Asif M., Hameed B.H., (2014), Preparation of mesoporous activated carbon from coconut frond for the adsorption of carbofuran insecticide, *Journal of Analytical and Applied Pyrolysis*, **110**, 172–180.

Nowicki P., Kazmierczak J., Pietrzak R., (2015), Comparison of physicochemical and sorption properties of activated carbons prepared by physical and chemical activation of cherry stones, *Powder Technology*, **269**, 312–319.

Saucier C., Adebayo M.A., Lima E.C., Cataluna R., Thue P.S., Prola L.D.T., Puchana-Rosero M.J., Machado F.M., Pavan F.A., Dotto G., (2015), Microwave-assisted activated carbon from cocoa shell as adsorbent for removal of sodium diclofenac and nimesulide from aqueous effluents, *Journal of Hazardous Materials*, **289**, 18–27.

Saygili H., Güzel F., (2016), High surface area mesoporous activated carbon from tomato processing solid waste by zinc chloride activation: Process optimization, characterization and dyes adsorption, *Journal of Cleaner Production*, **113**, 995–1004.

Seid A., Chouder D., Maouche N., Bakas I., Barka N., (2014), Removal of Cd(II) and Co(II) ions from aqueous solutions by polypyrrole particles: Kinetics, equilibrium and thermodynamics, *Journal of the Taiwan Institute of Chemical Engineers*, **45**, 2969–2974.

Shak K.P.Y., Wu T.Y., (2014), Coagulation–flocculation treatment of high-strength agro-industrial wastewater using natural *Cassia obtusifolia* seed gum: Treatment efficiencies and flocs characterization, *Chemical Engineering Journal*, **256**, 293–305.

Sbaffoni S., Boni M. R., Tedesco P, Vaccari M., (2018), Fe(II) and Mn(II) removal from contaminated groundwater by adsorption: a comparison of activated carbon and pine bark, *Environmental Engineering and Management Journal*, **17**, 1989-1999.

Soylak M., Narin I., Dogan M., (1997), Trace enrichment and atomic absorption spectrometric determination of lead, copper, cadmium and nickel in drinking water samples by use of an activated carbon column, *Analytical Letters*, **30**, 2801–2810.

Teklu T., Wangatia L.M., Alemayehu E., (2018), In situ deposition of polyaniline onto sisal fibers and removal efficiency for chromium (VI) from aqueous solution: Structure and adsorption studies, *Journal of Applied Surfaces and Interfaces*, **3**, 1–9.

Tounsadi H., Khalidi A., Abdennouri M., Barka N., (2016), Activated carbon from *Diplotaxis harra* biomass: Optimization of preparation conditions and heavy metal removal, *Journal of the Taiwan Institute of Chemical Engineers*, **59**, 348–358.

Tounsadi H., Khalidi A., Abdennouri M., Barka N., (2015), Biosorption potential of *Diplotaxis harra* and *Glebionis coronaria* L. biomasses for the removal of Cd(II) and Co(II) from aqueous solutions, *Journal of Environmental and Chemical Engineering*, **3**, 822–830.

Valero D., Garcia-Garcia V., Exposito E., Aldaz A., Montiel V., (2014), Electrochemical treatment of wastewater from almond industry using DSA-type anodes: Direct connection to a PV generator, *Separation and Purification Technology*, **123**, 15–22.

Vhahangwele M., Mugera G.W., (2015), The potential of ball-milled South African bentonite clay for 2 attenuation of heavy metals from acidic wastewaters: Simultaneous 3 sorption of Co^{2+}, Cu^{2+}, Ni^{2+}, Pb^{2+}, and Zn^{2+} ions, *Journal of Environmental Chemical Engineering*, **3**, 2416-2425.

Visa M., (2016), Synthesis and characterization of new zeolite materials obtained from fly ash for heavy metals removal in advanced wastewater treatment, *Powder Technology*, **294**, 338–347.

Wang Y.X., Ngo H.H., Guo W.S., (2015), Preparation of a specific bamboo based activated carbon and its application for ciprofloxacin removal, *Science of the Total Environment*, **533**, 32–39.

Wu Q., Tam N.F.Y., Leung J.Y.S., Zhou X., Fu J., Yao B., Huang X., Xia L., (2014), Ecological risk and pollution history of heavy metals in Nansha mangrove, South China, *Ecotoxicology and Environmental Safety*, **104**, 143–151.

Yahya M.A., Al-Qodah Z., Ngah C.W.Z., (2015), Agricultural bio-waste materials as potential sustainable precursors used for activated carbon production: A review, *Renewable and Sustainable Energy Reviews*, **46**, 218–235.

Zhang Z., Juying L., Mamat Z., Qing Fu Y., (2016a), Sources identification and pollution evaluation of heavy metals in the surface sediments of Bortala River, Northwest China, *Ecotoxicology and Environmental Safety*, **126**, 94–101.

Zhang L., Zeng Y., Cheng Z., (2016b), Removal of heavy metal ions using chitosan and modified chitosan: A review, *Journal of Molecular Liquids*, **214**, 175–191.

Zhu W.P., Gao J., Sun S.P., Zhang S., Chung T.S., (2015), Poly (amidoamine) dendrimer (PAMAM) grafted on thin film composite (TFC) nanofiltration (NF) hollow fiber membranes for heavy metal removal, *Journal of Membrane Science*, **487**, 117–126.